

Article

Generation and Validation of CFD-Based ROMs for Real-Time Temperature Control in the Main Control Room of Nuclear Power Plants

Seung-Hoon Kang, Dae-Kyung Choi , Sung-Man Son and Choengryul Choi * 

ELSOLTEC, #1401-2, BLDG A, 184, Jungbu-daero, Giheung-gu, Yongin-si 17095, Gyeonggi-do, Republic of Korea; shk@elsoltec.com (S.-H.K.); cdk@elsoltec.com (D.-K.C.); ssm@elsoltec.com (S.-M.S.)

* Correspondence: crchoi@elsoltec.com

Abstract: This study develops and validates a Reduced Order Model (ROM) integrated with Digital Twin technology for real-time temperature control in the Main Control Room (MCR) of a nuclear power plant. Utilizing Computational Fluid Dynamics (CFD) simulations, we obtained detailed three-dimensional thermal flow distributions under various operating conditions. A ROM was generated using machine learning techniques based on 94 CFD cases, achieving a mean temperature error of 0.35%. The ROM was further validated against two excluded CFD cases, demonstrating high correlation coefficients ($R > 0.84$) and low error metrics, confirming its accuracy and reliability. Integrating the ROM with the Heating, Ventilating, and Air Conditioning (HVAC) system, we conducted a two-month simulation, showing effective maintenance of MCR temperature within predefined criteria through adaptive HVAC control. This integration significantly enhances operational efficiency and safety by enabling real-time monitoring and control while reducing computational costs and time associated with full-scale CFD analyses. Despite promising results, the study acknowledges limitations related to ROM's dependency on training data quality and the need for more comprehensive validation under diverse and unforeseen conditions. Future research will focus on expanding the ROM's applicability, incorporating advanced machine learning methods, and conducting pilot tests in actual nuclear plant environments to further optimize the Digital Twin-based control system.

Keywords: reduced order model; computational fluid dynamics; real-time temperature control; HVAC system; nuclear power plant main control room; digital twin



Citation: Kang, S.-H.; Choi, D.-K.; Son, S.-M.; Choi, C. Generation and Validation of CFD-Based ROMs for Real-Time Temperature Control in the Main Control Room of Nuclear Power Plants. *Energies* **2024**, *17*, 6406. <https://doi.org/10.3390/en17246406>

Academic Editors: Marcin Sosnowski, Jaroslaw Krzywanski, Karolina Grabowska, Dorian Skrobek and Ghulam Moeen Uddin

Received: 1 October 2024
Revised: 30 October 2024
Accepted: 18 December 2024
Published: 19 December 2024



Copyright: © 2024 by the authors. Licensee MDPI, Basel, Switzerland. This article is an open access article distributed under the terms and conditions of the Creative Commons Attribution (CC BY) license (<https://creativecommons.org/licenses/by/4.0/>).

1. Introduction

Digital Twin (DT) technology has emerged as a crucial tool in optimizing and enhancing the operational efficiency of complex systems by precisely replicating physical systems within digital environments [1–3]. This replication facilitates various simulations, thereby improving the management and operational strategies of intricate systems. The applicability of DT is particularly pronounced in systems requiring high safety standards and complex operational procedures, such as nuclear power plant main control rooms (MCRs). By utilizing DT, scenarios that are challenging to implement in the physical world can be experimented with in virtual settings, thereby refining real-world operational and management strategies.

Recent advancements in sensor technology, Artificial Intelligence (AI), and the Internet of Things (IoT) have significantly expanded the feasibility of implementing DT. These technologies enable real-time data acquisition and processing, which are essential for the effective functioning of DT systems. In the context of nuclear power plant MCRs, the integration of these technologies holds substantial potential for real-time temperature monitoring and control within these complex infrastructures.

The MCR of a nuclear power plant serves as the central hub overseeing the operation of the reactor and other critical facilities. It is imperative to maintain accurate opera-

tional status awareness and control various systems effectively within the MCR. However, malfunctions or failures in temperature sensors within the MCR can lead to inaccurate temperature data acquisition, complicating the maintenance of optimal temperature levels. Such inaccuracies can impede efficient operations and timely responses. Additionally, variations in temperature distribution due to differing operational conditions and environments within the MCR may result in data from fixed-position sensors lacking representativeness.

To address these challenges, there is a need for technologies that can accurately capture real-time temperature information within the MCR and manage the operational and control systems efficiently based on more representative data. Computational Fluid Dynamics (CFD) analysis is valuable for understanding three-dimensional thermal and fluid flow distributions within the MCR. However, the computational speed and efficiency limitations of CFD pose challenges for real-time data acquisition.

To overcome these limitations, this study introduces a real-time data acquisition system utilizing a Reduced Order Model (ROM) derived from Computational Fluid Dynamics (CFD) analysis [4–7]. ROM technology streamlines complex engineering systems, significantly increasing simulation speeds and lowering computational costs. This approach has been instrumental in various engineering disciplines by accelerating design processes, cutting expenses, and enhancing performance, thereby fostering efficiency and innovation in contemporary engineering practices [8–11]. In aerospace engineering, ROM is applied to aerodynamic optimization and structural vibration analysis. In automotive engineering, it is used for vehicle dynamics simulation and engine performance improvement. In mechanical engineering, ROM accelerates finite element analysis and fluid dynamics simulations, while in energy engineering, it contributes to modeling renewable energy systems and analyzing power grid stability. Additionally, in control engineering, ROM is utilized for designing real-time control systems, and in civil and architectural engineering, it aids in predicting structural responses and assessing bridge safety. In biomedical engineering, ROM plays a crucial role in biomechanical modeling and optimizing drug delivery. Thus, ROM facilitates design time reduction, cost savings, and performance enhancements across various engineering fields, promoting efficiency and innovation in modern engineering.

The ultimate goal of this research is to develop ROMs based on CFD analysis for real-time monitoring of thermal and fluid flow distribution within the MCR of a nuclear power plant. This ROM will be used to continuously track environmental conditions and optimize the HVAC system to maintain optimal temperatures. The research involves designing a virtual MCR and HVAC system using existing data from nuclear power plants, conducting CFD simulations to capture three-dimensional thermal and fluid flow distributions under various conditions, and generating a validated ROM (Figure 1). The applicability of this ROM technology is then evaluated through its integration with the HVAC system. Figure 1 outlines the workflow, beginning with CFD simulations based on a 3D model of the MCR. The CFD data is used to train machine learning algorithms, leading to the creation of the ROM. Managed by the “Twin Builder” module, the ROM is deployed via a Python (3.1.0) application, enabling real-time interaction with the HVAC system. The “Twin Deployer” facilitates seamless integration, allowing the “Main Program (Controller)” to adjust HVAC operations based on virtual live sensor data. This closed-loop mechanism ensures efficient temperature control and air quality management. These processes aim to demonstrate the feasibility of a real-time temperature monitoring and control system, contributing to improved safety and efficiency in nuclear power plant control rooms.

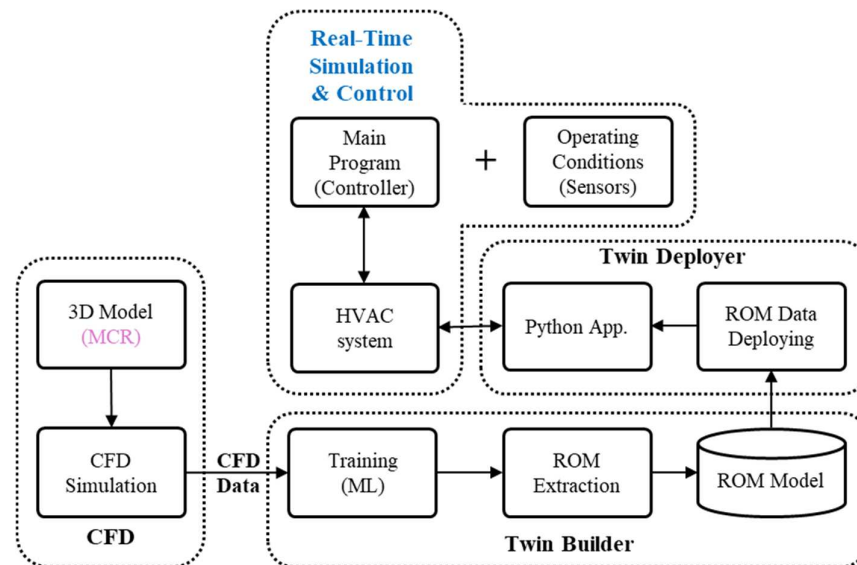


Figure 1. Workflow of CFD-based ROM generation and HVAC system applicability test.

2. Main Control Room and HVAC System

2.1. Main Control Room

The main control room (Main Control Room, MCR) of a nuclear power plant is a critical facility responsible for the operation and control of the reactor and associated systems, ensuring the stable and efficient functioning of the plant. The primary functions of the MCR include real-time monitoring of the reactor and systems, control operations, safety management, and communication. The MCR provides operators with a manual control interface through control panels and visualizes real-time data on monitoring displays, enabling rapid assessment of system status. The alarm system offers visual and auditory warnings during emergencies, facilitating swift responses, while the operator workstation is equipped with multiple monitors and control devices to support operational tasks. Emergency response equipment is available to handle urgent situations by providing the necessary tools in the event of an incident. The MCR is designed with system redundancy to maintain stable operations even during emergency scenarios and ensures the maintenance of optimal temperatures (21 °C to 25 °C) to guarantee the smooth functioning of equipment and a comfortable working environment for operators.

In this study, to obtain the three-dimensional thermal and fluid flow distribution within the MCR through Computational Fluid Dynamics (CFD) analysis, a virtual MCR was first designed by referencing existing data [12–22] from actual nuclear power plant main control rooms, as illustrated in Figure 2. This virtual MCR includes various heat-generating devices such as display units, computers, monitors, cabinets, servers, and printers, as well as HVAC systems (including Supply Diffusers and Return/Exhaust Grilles) and lighting fixtures. The ceiling is equipped with 38 Supply Diffusers and 24 Return/Exhaust Grilles, which supply and exhaust air to regulate pressure, temperature, and humidity. These installations play a crucial role in controlling the temperature and airflow within the MCR.

2.2. HVAC System

In this study, a conceptual HVAC (Heating, Ventilation, and Air Conditioning) system for a control room was designed based on data [12–22] from existing nuclear power plant control room HVAC systems and is illustrated in Figure 3. The control room HVAC system is responsible for the ventilation and air conditioning of various zones within the nuclear power plant, with normal operation airflows indicated by blue lines.

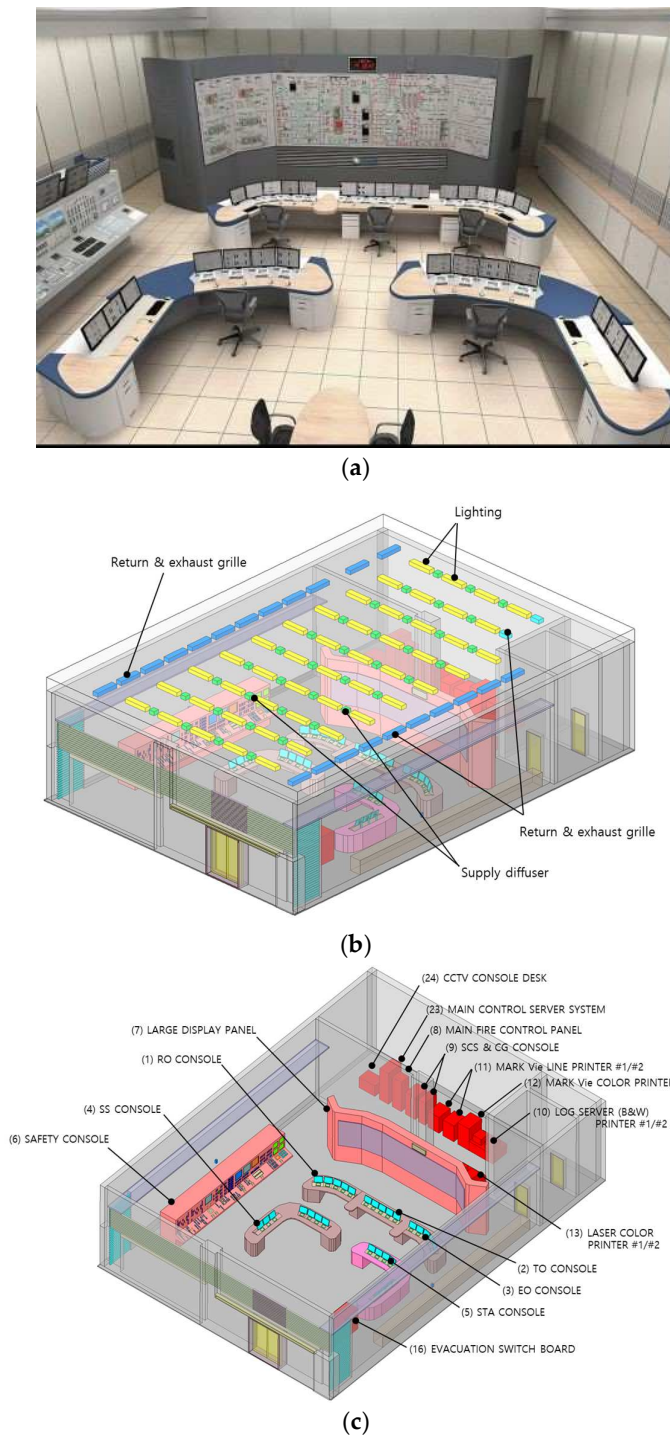


Figure 2. Virtual main control room (MCR). (a) Image of MCR; (b) Supply diffusers and return/exhaust grilles; (c) Devices and equipment.

The basic configuration of the HVAC system begins with the intake of external air through the Outside Air Intake, which is then conveyed via a concrete tunnel designed for missile protection to the Supply Air Handling Unit. The Supply AHU, installed at the front of each compartment, supplies conditioned air to the Main Control Room (MCR), Technical Support Center (TSC), Computer Room, HVAC equipment room, restrooms, and kitchen areas. If the temperature obtained from the internal temperature sensors of the MCR exceeds the design standard, the system cools the air through heat exchange with seawater. Conversely, if the temperature is below the standard, heaters are activated to

raise the supply air temperature. The vertical pump for seawater cooling is depicted on the right side of the figure.

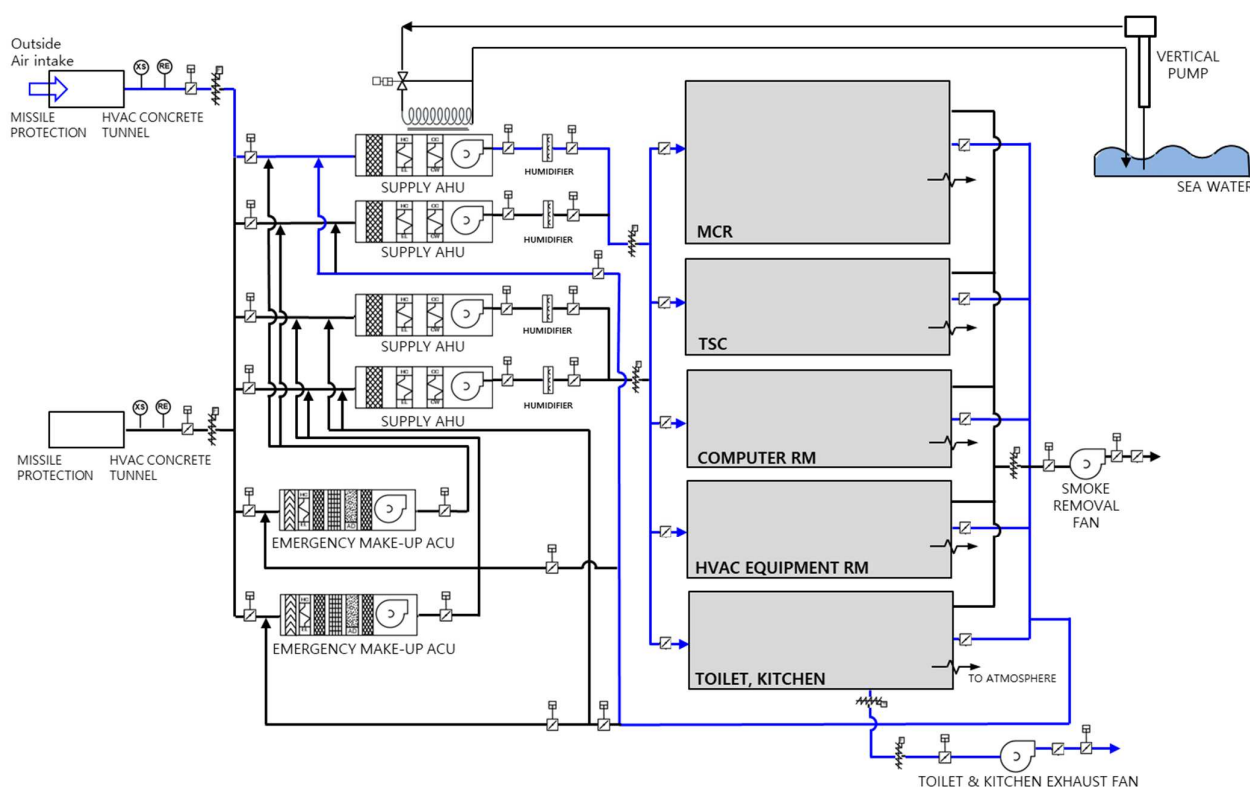


Figure 3. HVAC system for the MCR of the virtual nuclear power plant (blue line during normal operation).

Under normal operation, most of the air supplied to each compartment is recirculated and merges with the Outside Air Intake, allowing the air to continuously circulate within the HVAC system to maintain temperature and humidity levels. A portion of the air supplied to the restrooms and kitchen is exhausted to the atmosphere through the Toilet and Kitchen Exhaust Fan. A small fraction of the supplied air leaks through the doors and penetrations of each compartment, which helps maintain slightly higher pressure within each compartment.

The Emergency Make-up Air Conditioning Unit (Emergency Make-up ACU) functions as an auxiliary ventilation device to intake additional external air during emergency situations, operating immediately when needed to supplement the air supply. Additionally, the Smoke Removal Fan is designed to expel smoke from compartments during emergencies such as fires, ensuring a safe ventilation environment within the control room and TSC.

3. CFD Analysis

To obtain the three-dimensional thermal flow distribution under various operating conditions within the control room, a three-dimensional Computational Fluid Dynamics (CFD) analysis was performed. This involved creating a three-dimensional CAD model of the control room, defining the flow analysis domain, and generating the CFD mesh. Subsequently, the CFD analysis was conducted by applying various boundary conditions to the mesh, resulting in the thermal flow distribution within the control room under different operating scenarios.

3.1. Model and Conditions of CFD Analysis

In this study, a conceptual control room was designed based on data [12–22] from existing nuclear power plant control rooms, as illustrated in Figure 2. Utilizing this design,

a three-dimensional CAD model of the control room was created, the flow analysis domain was defined, and the CFD mesh was generated, as shown in Figure 4. After conducting a mesh sensitivity evaluation using three grid levels: coarse, intermediate, and fine (current grid), the final mesh used for the analysis comprised 8,991,000 cells. During mesh generation, regions near the HVAC system and heat-generating equipment, where significant variations in physical quantities were expected, were assigned a finer mesh to enhance the accuracy of the analysis.

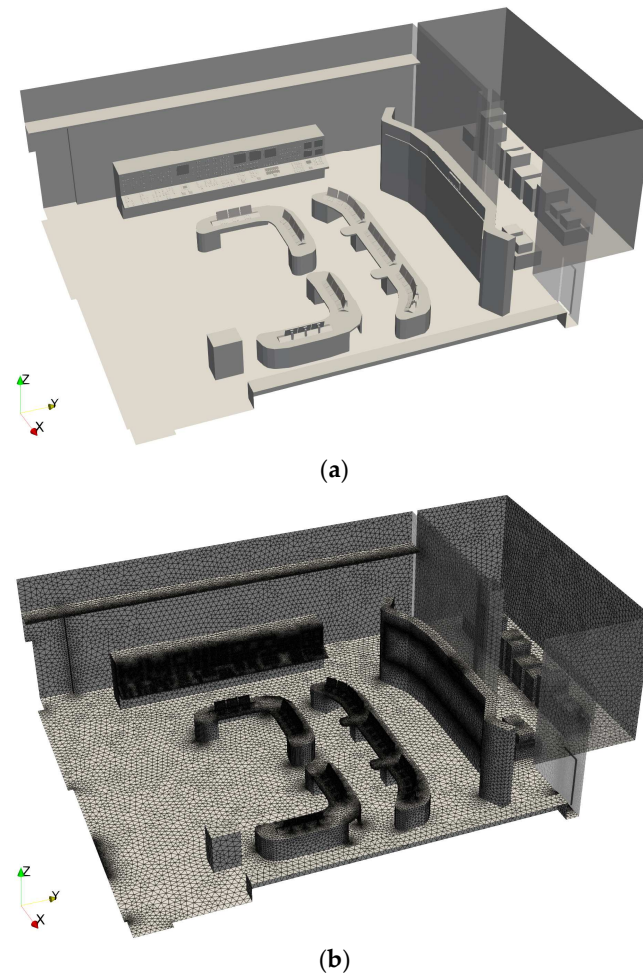


Figure 4. 3D model and mesh system of the MCR for CFD analysis. (a) 3D model; (b) Mesh system.

To establish the CFD analysis conditions, the operating conditions of the conceptual control room were designed based on data [12–22] from existing nuclear power plant control rooms and summarized in Table 1. Initially, the airflow rates and temperatures at the Supply Diffusers and Return/Exhaust Grilles, the heat transfer through the walls, the heat generation from equipment and devices, and additional heat loads were determined.

Based on these parameters, the range of variation for each category was established, and the specific variation amounts and values to be applied in the CFD analysis were determined. By combining these factors, a total of 96 CFD analysis conditions were established.

The airflow rates of the Supply Diffusers were set within a range of 20,732 to 24,650 CMH, resulting in two selected conditions, while the supply air temperatures were varied across nine conditions from 10.0 °C to 30.0 °C. The airflow rates for the Return/Exhaust Grilles were selected within the same range as the Supply Diffusers. The heat transfer through the walls was fixed based on the conditions of adjacent compartments, with the heat transfer rates for the

floor, east, west, south, north, and ceiling set at 5.1 kW, 0.9 kW, 6.5 kW, 0.3 kW, −0.2 kW, and 6.7 kW, respectively. The total wall heat transfer was referred to as Heat Transfer Through Walls.

Table 1. Design values and various operating conditions (CFD analysis cases).

		Unit	Design	Range	No. of Selected Operating Conditions [EA]	No. of Combined Operating Conditions for CFD [EA]
Supply Diffusers (38 EA)	Flow rate	[CMH]	24,650	20,732 ~24,650	2	96
	Temperature	[°C]	20	10.0 ~ 30.0	9	
Return/Exhaust Grilles (24 EA)	Flow rate	[CMH]	24,650	20,732 ~ 24,650	2	
Wall (Transmission)	Floor	[kW]	5.1	Fixed	1	
	East	[kW]	0.9	Fixed	1	
	West	[kW]	6.5	Fixed	1	
	South	[kW]	0.3	Fixed	1	
	North	[kW]	−0.2	Fixed	1	
	Ceiling	[kW]	6.7	Fixed	1	
Heat Load I	I&C Equip.	[kW]	30.2	24.7 ~ 42.7 kW (82 ~ 141%)	7	
	Elect. Load	[kW]	3.3	Fixed	1	
	Operator	[kW]	0.6	Fixed	1	
Heat Load II	Add. Heat	[kW]	0	0.0 ~ 20.0 kW	3	
SUM			53.4	47.9 ~ 85.9 kW	-	

The heat load from equipment and devices (I&C Equipment) varied within a range, with a baseline value of 30.2 kW (design value) and selected across seven conditions from 24.7 kW to 42.7 kW (82% to 141% of the design value). The electrical load was fixed at 3.3 kW, and the heat load from operators was fixed at 0.6 kW. The sum of these was referred to as Heat Load I. Additional heat loads (Heat Load II) were selected across three conditions ranging from 0 kW to 20 kW.

To capture the thermal flow distribution under various operating conditions within the MCR, these parameters were combined to establish a total of 96 CFD analysis conditions. To address the potential issue of having an excessive number of cases from fully combining all four variables, a strategic approach was taken to limit the analysis to 96 cases. If all four variables were fully combined, it would result in 378 scenarios, which would be impractical for thorough CFD analysis due to the extensive computational resources required. Therefore, to effectively capture the impact of each variable while maintaining a manageable number of cases, 96 cases were selected. This selection was done by carefully combining the variables, ensuring that the key variations in airflow rates, temperatures, and heat loads were adequately covered. By doing so, the analysis could still provide insights into the thermal distribution under different operating conditions without needing to evaluate every possible combination. This approach strikes a balance between thoroughness and feasibility in the CFD analysis.

Representative analysis cases and their corresponding conditions are presented in Table 2. Case 01 represents a standard operational scenario and will be used directly in the ROM generation process. It serves as a baseline case that captures typical thermal behavior under normal conditions. Case 06 and Case 52, on the other hand, are selected not for ROM generation but for the verification of the ROM. Case 06 reflects cooler operating conditions with lower diffuser temperatures, while Case 52 represents a scenario with reduced airflow. By using these cases for verification, the ROM's ability to accurately predict thermal behavior under different conditions can be validated.

Table 2. Represented CFD analysis cases.

Case	Supply Diffusers		Heat Load					Total [kW]
	Flow Rate [CMH]	Temp. [K]	Heat Load I			Heat Load II		
			Wall [kW]	I&C Equip. [kW]	Elect. Load [kW]	Operator [kW]	Add. Heat [kW]	
01	24,650	303.15	19.3	30.2	3.3	0.6	0	53.4
06	24,650	290.65	19.3	30.2	3.3	0.6	0	53.4
52	20,732	295.65	19.3	30.2	3.3	0.6	0	53.4

3.2. Methodology of CFD Analysis

To obtain the three-dimensional thermal flow distribution under various operating conditions within the control room, CFD analyses were performed for a total of 96 different operating condition scenarios, as outlined in Tables 1 and 2. The governing equations used to determine the airflow and temperature distribution within the control room included the continuity equation, the momentum equations (Navier–Stokes Equations), and the energy equation. To account for turbulent flow characteristics, the standard k– ϵ model, which is widely used in turbulence modeling, was employed [23]. The CFD analyses were conducted using ANSYS FLUENT (ver. 19) [24,25], performing steady-state simulations for each set of analysis conditions. The density variation of air with temperature was modeled using the Boussinesq Approximation.

Supply diffusers were set as Velocity Inlets, while among the Return/Exhaust Grilles, one was configured as a Pressure Outlet, and the remaining were set as Outflows (with Velocity Inlet conditions indicating flow exiting from the Main Control Room, MCR). Heat loads for the control room walls, floor, ceiling, I&C equipment, and electrical loads were applied as Wall Heat Fluxes, whereas heat from operators and additional heat loads were treated as Volume Heat Sources within the respective regions. During the analysis, velocities, temperatures, and pressures were monitored at two temperature sensor locations and 94 monitoring points, and the airflow rates and temperatures were monitored at the Return/Exhaust Grilles.

In ANSYS FLUENT, the SIMPLE algorithm was utilized for pressure-velocity coupling, and a second-order upwind scheme was employed for the spatial discretization of each equation [24,25]. This higher-order numerical scheme improves the precision of the solution by reducing numerical diffusion and better-capturing gradients in the flow variables, thereby contributing to the overall reliability of the CFD results. The convergence criterion was set such that the residuals for all variables were reduced below 10^{-3} . This rigorous convergence criterion guarantees the stability and precision of the CFD simulations. For 96 analysis conditions, as shown in Tables 1 and 2, the maximum error between the average temperature at the outlet (return and exhaust grilles) calculated from the thermal equilibrium perspective and the CFD analysis result was less than about 0.11%, confirming the reliability of the CFD analysis result.

3.3. Results of CFD Analysis

To obtain the three-dimensional thermal flow distribution under various operating conditions within the control room, CFD analyses were conducted for a total of 96 different operating condition scenarios, as outlined in Tables 1 and 2. Among these, the airflow and temperature distribution within the control room for Case 01 are presented in Figure 5.

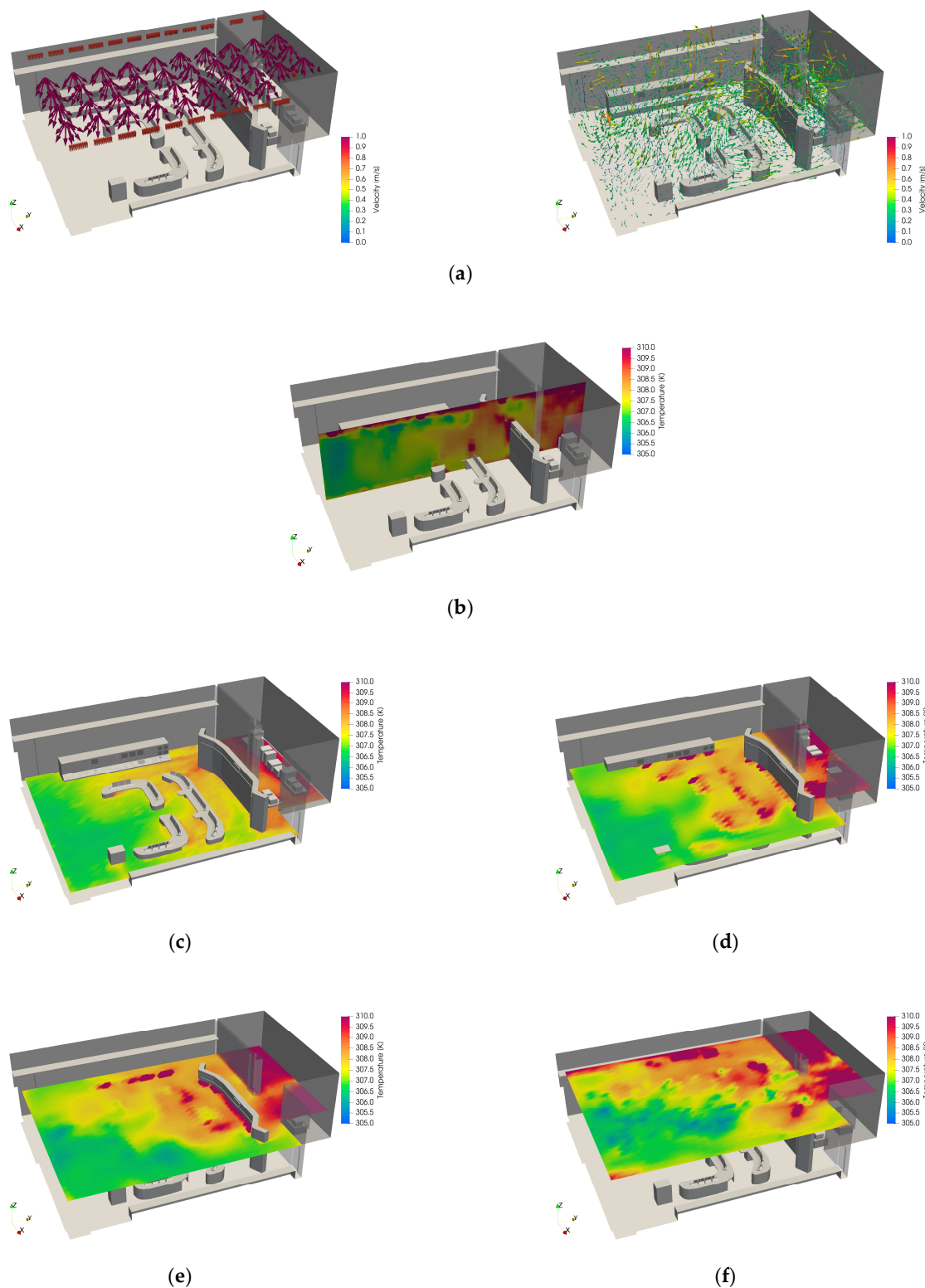


Figure 5. CFD results of Case 01. (a) Velocity vectors; (b) Temperature (vertical section); (c) Temperature (horizontal section: 0.5 m); (d) Temperature (horizontal section: 1.37 m); (e) Temperature (horizontal section: 2.5 m); (f) Temperature (horizontal section: 4.1 m).

Figure 5a presents the airflow patterns within the MCR. The left image shows the velocity vectors at the supply diffusers and return/exhaust grilles, illustrating how air is introduced and removed from the room. The vectors reveal concentrated air discharge and exhaust, helping regulate the room's ventilation. The right image depicts the resulting

airflow throughout the MCR when air is supplied and exhausted at these points. It provides an overview of air circulation, highlighting efficient flow areas and potential zones of stagnant air and offering insights into the HVAC system's performance. The airflow is closely related to temperature distribution because moving air transfers heat across the room. Proper airflow ensures an even mixing of warm and cool air, preventing temperature imbalances. Effective ventilation helps maintain a consistent temperature by cooling warm areas and distributing heat evenly, which is essential for the MCR's comfort and operational efficiency.

Figure 5b depicts the temperature distribution in a vertical cross-section of the control room, while Figure 5c–f show the temperature distributions in horizontal cross-sections at different heights (0.5 m, 1.37 m, 2.5 m, and 4.1 m, respectively). From Figure 5b, the vertical variation of temperature distribution due to airflow can be observed, particularly noting an increase in temperature towards the upper regions. This phenomenon is associated with natural convection effects, where warmer air rises and cooler air descends.

The horizontal cross-sections in Figure 5c–f display the temperature distributions at various heights within the control room. Clear differences in temperature distribution are evident with height, especially showing significant temperature increases in areas concentrated with heat sources. Figure 5c shows the temperature distribution in the lower section of the control room at a height of 0.5 m, where temperatures are relatively uniformly distributed. In contrast, Figure 5d reveals locally elevated temperatures in specific areas at a height of 1.37 m, which can be attributed to the influence of equipment or heat sources. Figure 5e clearly shows the temperature distribution at a height of 2.5 m, and Figure 5f shows higher temperature regions, primarily in areas with heat sources located at the upper part of the control room at a height of 4.1 m.

These results demonstrate the typical characteristics of airflow and temperature distribution within the control room. As mentioned in Section 1 of this paper, the thermal flow distribution within the control room varies depending on the location, thereby proving that temperature information obtained from only one or two temperature sensors installed at limited locations cannot represent the overall temperature distribution within the control room.

A total of 96 CFD analyses were conducted, including Case 01 presented in Figure 5, and all results exhibited similar airflow and temperature distributions as observed in Case 01. Each CFD analysis required approximately 24 h on a 40-core computer.

4. ROM Generation and Validation

In this study, a Reduced Order Model (ROM) was developed by training a Machine Learning (ML) model using thermal flow distribution data obtained from Computational Fluid Dynamics (CFD) analyses under various operating conditions within the nuclear power plant control room as detailed in Section 3. The accuracy of the ROM was subsequently validated to ensure its reliability.

4.1. ROM

A Reduced Order Model (ROM) is a technique that simplifies a complex, multidimensional system into a lower-dimensional representation to enhance computational efficiency. This approach is particularly significant in CFD analyses, where simulations accurately capture intricate physical phenomena such as fluid flow and heat transfer but are often hindered by high computational costs and long processing times. ROM effectively reduces high-dimensional data while preserving essential dynamic characteristics, enabling rapid analyses.

The ROM construction process typically involves the following stages: data collection, dimensionality reduction, low-dimensional model creation, and validation and calibration. Initially, high-dimensional CFD simulation data from various operating conditions are collected. Dimensionality reduction techniques such as Proper Orthogonal Decomposition (POD), Principal Component Analysis (PCA), or Singular Value Decomposition (SVD) are

then applied to extract the dominant modes [26,27]. Based on these modes, the system is reconstructed in a low-dimensional space. The model's accuracy is subsequently verified and calibrated using additional simulation or experimental data.

The implementation of ROM offers substantial benefits, including accelerated computational performance, decreased memory requirements, and suitability for real-time applications. These advantages have facilitated the extensive adoption of ROM across multiple industries, such as aerospace, automotive, energy, and medical engineering, where it is employed for real-time flow analysis, optimization, and design support [3–11]. Additionally, recent advancements have focused on integrating machine learning and artificial intelligence techniques to further enhance the accuracy and adaptability of ROMs.

4.2. ROM Generation

In this study, the CFD results for the control room, as described in Section 3, were utilized to generate the ROM. Commercial software ANSYS Twin Builder (2023R1) was employed, specifically using the Static ROM Builder. The Static ROM Builder approximates solutions in real-time for specific sets of parameters by compressing the solution using Singular Value Decomposition (SVD) and combining it with interpolation methods to recalculate values within the parameter range [26,27].

Four input parameters were used to create the ROM: the airflow rate and temperature supplied by the control room's HVAC system and the heat generation from equipment and compartments (Table 1). To enhance the reliability of the Static ROM, the CFD analysis cases used as training data were carefully selected to include the maximum and minimum ranges of the analysis parameters, utilized more than ten data points per parameter, and avoided excessive data usage for specific conditions [28]. Given the complex airflow expected due to the diverse equipment installed in the control room, approximately 94 CFD analysis results were used as training data, which are significantly more than the recommended minimum of ten per parameter.

Out of the total 96 CFD analysis cases presented in Table 1, 94 cases were used as training data to develop the Static ROM, while the remaining two cases were reserved for validating the generated ROM model. During the ROM creation process, parameters such as pressure, temperature, velocity, and vector fields from the CFD results were used. Separate ROMs were generated for each parameter, applying a 14-mode reduction where both reduction and leave-one-out Root Mean Square (RMS) errors were optimized. The total number of points used in the ROM was 8,991,000, matching the grid system employed in the CFD analysis. The average relative error for temperature in the ROM was found to be 0.35%.

To simultaneously calculate the four parameters (pressure, temperature, velocity, and vector), individual ROMs were first created for each parameter, as depicted in Figure 6. These ROMs were then integrated into a single Twin model. Additionally, to facilitate the integration of the Twin model with the entire HVAC system of the control room, the Twin model was exported as Python code. This process involved combining the ROMs for each parameter generated in ANSYS Twin Builder into a unified Twin model and using ANSYS Twin Deployer to generate the Python code, as illustrated in Figure 7. Similar to the CFD analysis, all 96 operating conditions were applied, and Python code was generated based on the analyzed results.

The computation time for the four Static ROMs generated was below one second, demonstrating a significantly faster calculation speed compared to the original CFD analyses.

4.3. ROM Validation

To validate the generated ROM, the CFD analysis results and ROM calculation results for Case 01 (included in the ROM training dataset) and Cases 06 and 52 (excluded from ROM training) are presented together in Figure 8. In each subfigure, the left panel displays the CFD analysis results, while the right panel shows the corresponding ROM calculation results. The color gradients and vector fields represent the temperature distribution and

velocity vectors within the modeled space, respectively, allowing for a direct comparison between the two models.

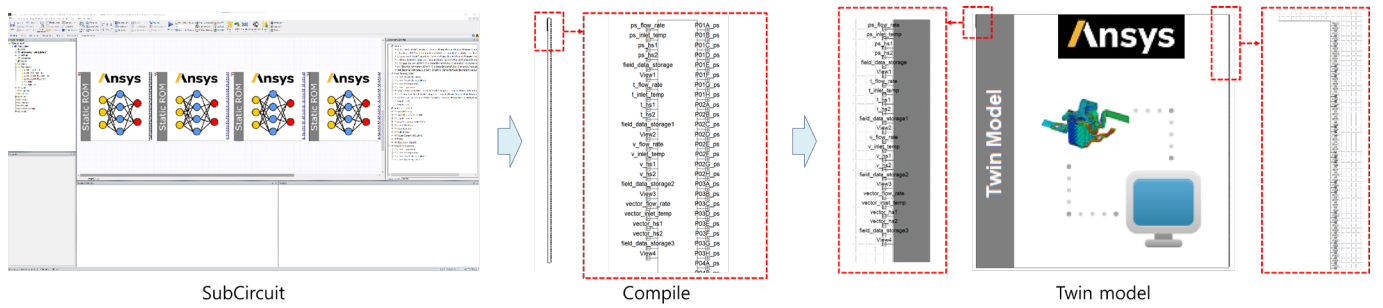


Figure 6. Process of creating the Twin model incorporating four parameter order reduction models.

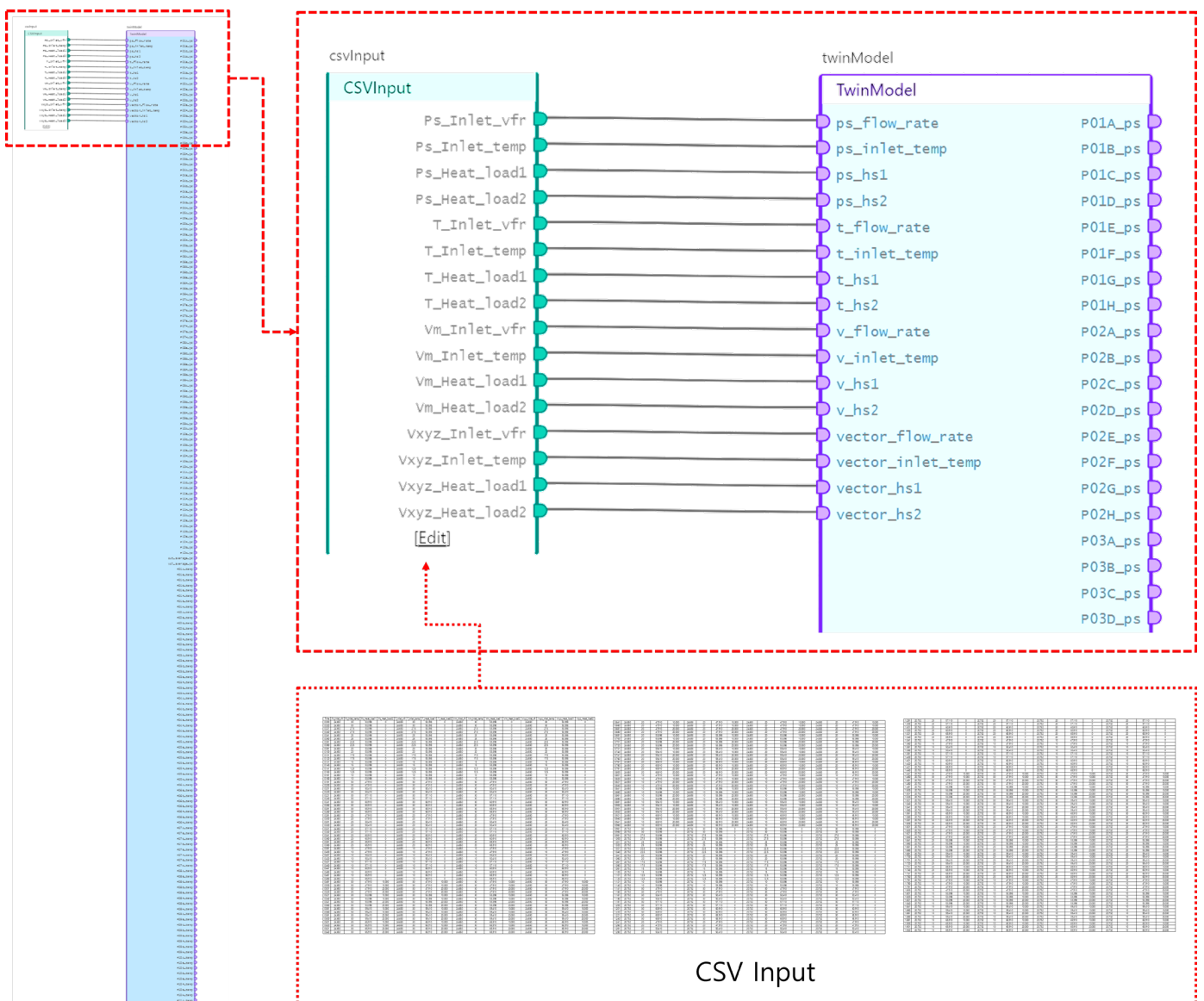


Figure 7. Modeling for the system in the ANSYS Twin Deployer.

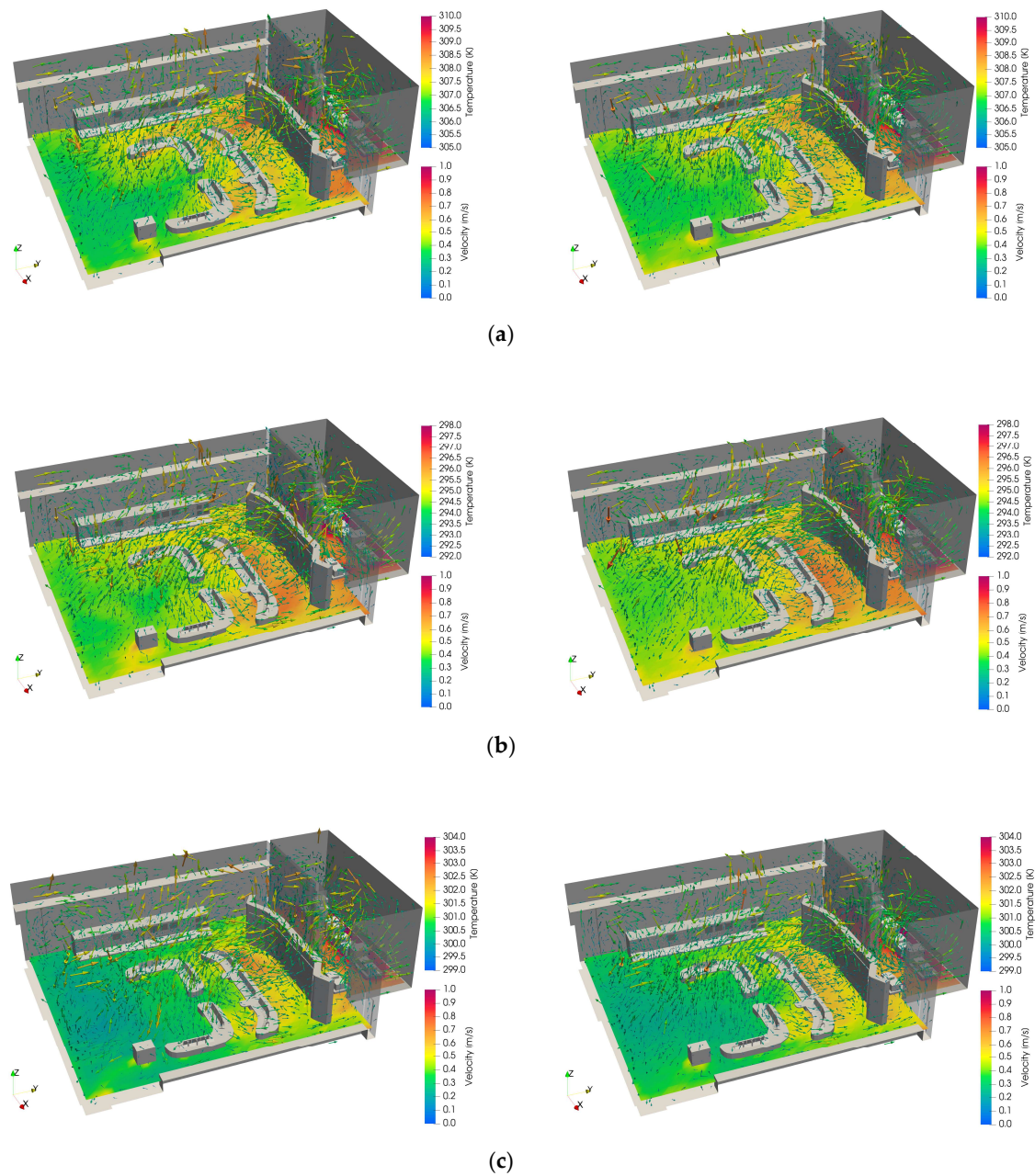


Figure 8. Comparison of CFD and ROM results ((Left): CFD, (Right): ROM). (a) Case 01; (b) Case 06; (c) Case 52.

Figure 8a illustrates Case 01, which is part of the ROM training dataset. The CFD and ROM results exhibit highly similar trends in both temperature distribution and velocity patterns. This similarity indicates that the ROM can accurately reproduce CFD analysis results within the parameter range used for training, thereby demonstrating the ROM's reliability.

Figure 8b presents Case 06, a validation case excluded from the ROM training dataset. The ROM calculation results show a high degree of agreement with the CFD results in the major flow regions. Although slight discrepancies are observed in localized velocity magnitudes and temperature distributions, the ROM effectively captures the overall flow trends and maintains high predictive performance even for cases not included in the training dataset.

Figure 8c shows Case 52, another validation case excluded from ROM training. The comparison between CFD and ROM results confirms the ROM's predictive performance,

with consistent temperature and velocity distributions observed between the two models. Minor differences are present in areas with complex flow patterns, but overall, the ROM successfully approximates the CFD analysis results.

In addition to the qualitative comparison presented in Figure 8, a quantitative comparison is summarized in Table 3 for the three cases (Case 01, Case 06, and Case 52). Table 3 provides a quantitative assessment by comparing the maximum, minimum, mean, and standard deviation values of velocity magnitudes and temperatures between CFD and ROM results. Similarity metrics such as Reduced Difference (RD), Root Mean Square Error (RMSE), Mean Absolute Error (MAE), and the correlation coefficient (R) were used to analyze the differences between the two models.

Table 3. Comparison of CFD and ROM results.

		Case 01				Case 06				Case 52			
		Velocity Mag. [m/s]		Temperature [K]		Velocity Mag. [m/s]		Temperature [K]		Velocity Mag. [m/s]		Temperature [K]	
		CFD	ROM	CFD	ROM	CFD	ROM	CFD	ROM	CFD	ROM	CFD	ROM
Max Value		3.06	2.92	472.83	468.99	3.05	3.01	468.38	462.62	459.28	470.46	459.28	470.46
Min Value		0.01	−0.01	303.15	302.47	0.00	0.03	290.65	290.57	295.63	295.89	295.63	295.89
Mean Value		0.25	0.24	308.68	308.79	0.25	0.26	296.47	296.37	302.32	302.44	302.32	302.44
Standard Deviation		0.17	0.18	3.28	3.28	0.17	0.18	3.38	3.25	3.33	3.36	3.33	3.36
Similarity	RD [-]	0.225		0.001		0.370		0.002		0.352		0.001	
	RMSE [m/s] or [K]	0.074		0.805		0.090		1.000		0.085		0.990	
	MAE [m/s] or [K]	0.042		0.393		0.059		0.461		0.058		0.447	
	R [-]	0.910		0.970		0.867		0.956		0.846		0.957	

For Case 01, both the maximum and mean values of velocity magnitudes and temperatures are similar between CFD and ROM results, with no significant differences in standard deviations. The RD and RMSE values are 0.225 and 0.074 m/s for velocity magnitudes and 0.001 and 0.805 K for temperatures, respectively, indicating a high degree of precision in the ROM's replication of CFD results. The MAE values are 0.042 m/s for velocity magnitudes and 0.393 K for temperatures, showing minimal discrepancies. The correlation coefficient R is 0.910, demonstrating a strong correlation between the two models.

In the validation Case 06, slight differences are observed in both velocity magnitudes and temperatures between CFD and ROM results. The RD and RMSE values are 0.370 and 0.090 m/s for velocity magnitudes and 0.002 and 1.000 K for temperatures, respectively, indicating relatively low differences. The MAE values are 0.059 m/s for velocity magnitudes and 0.461 K for temperatures, showing good agreement. The correlation coefficients R are 0.867 for velocity magnitudes and 0.956 for temperatures, confirming a high level of correlation between the models.

For Case 52, the maximum and mean values of velocity magnitudes and temperatures are similar between CFD and ROM results, with comparable standard deviations. The RD and RMSE values are 0.352 and 0.085 m/s for velocity magnitudes and 0.001 and 0.990 K for temperatures, respectively, indicating small errors. The MAE values are 0.058 m/s for velocity magnitudes and 0.447 K for temperatures, showing minimal discrepancies. The correlation coefficients R are 0.846 for velocity magnitudes and 0.957 for temperatures, maintaining a high correlation between the models.

The correlation coefficient (R) for velocity is slightly lower compared to that for temperature. This lower correlation in velocity is primarily due to the presence of regions with inherently low velocities within the analysis domain, which affects the overall correlation metrics. The similarity between CFD and ROM results for temperature is sufficiently high,

demonstrating that the ROM effectively captures the essential thermal dynamics relevant to practical operations.

Overall, the combined qualitative and quantitative results presented in Figure 8 and Table 3 confirm that the ROM accurately predicts CFD results across all three examined cases. While minor discrepancies exist in the RD, RMSE, and MAE metrics, the overall high correlation coefficients indicate that the ROM effectively captures the essential airflow and temperature distribution patterns. This validation demonstrates that the ROM not only enhances computational efficiency but also maintains a high level of accuracy, making it a reliable alternative for fluid dynamics analysis within the control room environment. Notably, the ROM demonstrates robust predictive capabilities not only for the training cases but also for validation cases excluded from the training dataset. Although some discrepancies are observed in specific regions due to the simplified nature of the ROM compared to the detailed CFD model, the ROM nonetheless provides a reliable alternative that balances computational efficiency with accuracy in fluid dynamics analysis.

5. Applicability Test of ROM in Combination with HVAC System

Finally, the applicability of the generated ROM was verified by integrating it with the control room's HVAC system.

5.1. HVAC System Operating Conditions

To validate the applicability of the generated ROM in combination with the control room HVAC system, the operating conditions of the virtual nuclear power plant control room HVAC system, as illustrated in Figure 2, were designed and summarized in Table 4. The table presents conditions related to the external air intake, recirculated air, air handling unit (AHU) performance, heat loads, and airflow conditions for each zone. The external air intake flow rate was fixed at 6600 CMH, with temperatures ranging from $-13.2\text{ }^{\circ}\text{C}$ to $16.3\text{ }^{\circ}\text{C}$. Recirculated air was maintained at 35,240 CMH to regulate indoor temperature and humidity. The Supply AHU exhibited cooling and heating capacities of up to 150 kW and 50 kW, respectively, and was controlled in multiple stages based on temperature variations. Airflow in the Main Control Room (MCR) was managed by supply diffusers and return grilles, maintaining flow rates of 24,650 CMH and 24,283 CMH, respectively. Heat loads were determined by wall conduction, equipment, and operator activities, with Instrumentation and Control (I&C) equipment generating heat loads ranging from 20.80 kW to 38.50 kW. Airflow and heat loads for other areas, including the Technical Support Center (TSC), Computer Room, HVAC equipment room, restrooms, and kitchen, were presented with fixed flow rates and leakage based on their specific characteristics. These conditions were designed to ensure appropriate airflow and heat management in the MCR and each zone, thereby guaranteeing safe operation.

Figure 9 illustrates the temporal variations in the operating conditions of the nuclear power plant control room HVAC system. This figure is based on a virtually designed scenario to verify the applicability of the integrated HVAC system and ROM in maintaining the control room temperature within acceptable levels despite changes in external air temperature and heat loads. The external intake air temperature varies from $-13.2\text{ }^{\circ}\text{C}$ to $16.3\text{ }^{\circ}\text{C}$, reflecting environmental changes that significantly impact heating and cooling loads. Heat Load I comprises loads from Instrumentation and Control (I&C) equipment, electronic devices, and operators, varying within a range of 24.7 kW to 42.4 kW. Notably, the I&C equipment serves as the most influential factor, while the loads from other elements remain relatively stable. Heat Load II, resulting from additional heat sources, fluctuates irregularly within a range of 0 kW to 20 kW, influenced by changes in external conditions and operational situations. This variability is a critical factor in assessing the responsiveness of the HVAC system. The total heat load is the sum of Heat Load I and Heat Load II, varying between 40.0 kW and 80.3 kW. This range evaluates whether the HVAC system can reliably respond to total heat load variations and effectively control the temperature within the control room. Through this evaluation, the study verifies that the MCR

HVAC system integrated with the ROM operates appropriately under diverse heat loads and external condition changes.

Table 4. Conditions for HVAC system applicability test.

		Unit	Value	Remark		
Outside Air In-take(Atmosphere)	Flow Rate	[CMH]	6600	Fixed		
	Temperature	[°C]	− 13.2 ~ 16.3	Variable over time (Figure 9a)		
Recirculation	Flow Rate	[CMH]	35,240	Fixed		
	Temperature	[°C]	-	Calculated from HVAC system		
Supply AHU	Flow Rate	[CMH]	41,840	Fixed		
	Performance	Cooling	[kW]	Max. 150	- Controlled based on MCR Temperature - 15 Levels (Interval 10 kW)	
		Heating	[kW]	Max. 50	- Controlled based on MCR Temperature - 5 Levels (Interval 10 kW)	
	Control	[-]	On	-		
MCR	Flow Rate	Supply Diffusers (38 EA)	[CMH]	24,650	Fixed	
		Return Grilles (24 EA)	[CMH]	24,283	Fixed	
		Leakage	[CMH]	367	Fixed	
	Heat Load	Wall (Transmission)	Floor	[kW]	5.10	Fixed
			East	[kW]	0.90	Fixed
			West	[kW]	6.50	Fixed
			South	[kW]	0.30	Fixed
			North	[kW]	−0.20	Fixed
			Ceiling	[kW]	6.70	Fixed
	Heat Load I		I&C Equip.	[kW]	20.80 ~ 38.50	Variable over time (Figure 9b)
			Elect. Load	[kW]	3.30	Fixed
			Operator	[kW]	0.60	Fixed
			Heat Load II	Add. Heat	[kW]	0.00 ~ 20.00
TSC	Flow Rate	Supply Diffusers	[CMH]	5035	Fixed	
		Return Grilles	[CMH]	4790	Fixed	
		Leakage	[CMH]	245	Fixed	
	Heat Load	[kW]	6.873	Fixed		
Computer Room	Flow Rate	Supply Diffusers	[CMH]	490	Fixed	
		Return Grilles	[CMH]	0	Fixed	
		Leakage	[CMH]	490	Fixed	
	Heat Load	[kW]	0.165	Fixed		
HVAC Equipment Room	Flow Rate	Supply Diffusers	[CMH]	2701	Fixed	
		Return Grilles	[CMH]	991	Fixed	
		Leakage	[CMH]	1710	Fixed	
	Heat Load	[kW]	4.559	Fixed		
Toilet, Kitchen	Flow Rate	Supply Diffusers	[CMH]	8964	Fixed	
		Return Grilles → Return Duct	[CMH]	5176	Fixed	
		Exhaust Grilles → Exhaust FAN → Atmosphere	[CMH]	3178	Fixed	
	Leakage	[CMH]	610	Fixed		
Heat Load	[kW]	12.085	Fixed			

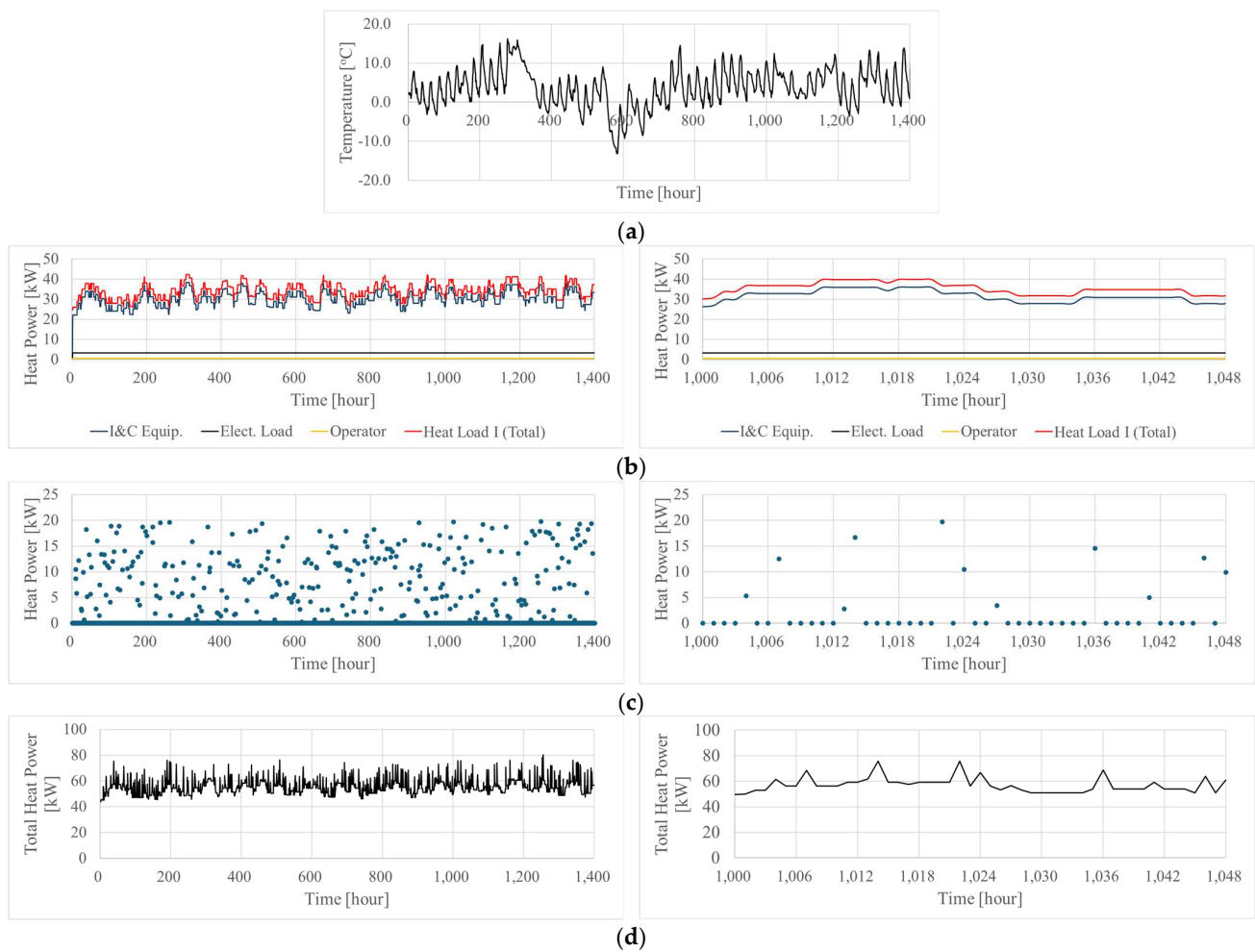


Figure 9. Condition variables over time for HVAC system applicability test. (a) Intake air temperature ($-13.2 \sim 16.3$ °C); (b) Heat Load I ($24.7 \sim 42.4$ kW); (c) Heat Load II ($0.0 \sim 20.0$ kW); (d) Total Heat Load ($40.0 \sim 80.3$ kW).

5.2. Methodology of Applicability Test

To verify the applicability of the generated ROM in controlling the temperature of the control room HVAC system in the virtual nuclear power plant, a separate simulation program was developed (Figures 1 and 3). Using this simulation program, virtual simulation calculations were performed over a period of approximately two months by applying the MCR HVAC system presented in Figure 3, along with the operating conditions outlined in Table 4 and Figure 9.

In the simulation, acquiring temperature data from the sensor locations for each loop calculation took less than one second, while obtaining the entire three-dimensional thermal flow distribution required under ten seconds. These simulation results were used to evaluate whether the integration of the control room HVAC system with the ROM could effectively manage the control room temperature under various operating conditions and heat load variations.

5.3. Results of Applicability Test

The results of the applicability test, where the ROM was integrated with the nuclear power plant control room HVAC system, are presented in Figure 10. The graphs illustrate the temperature variations within the control room and the corresponding changes in the cooling and heating performance of the Supply AHU that were controlled to maintain these temperatures.

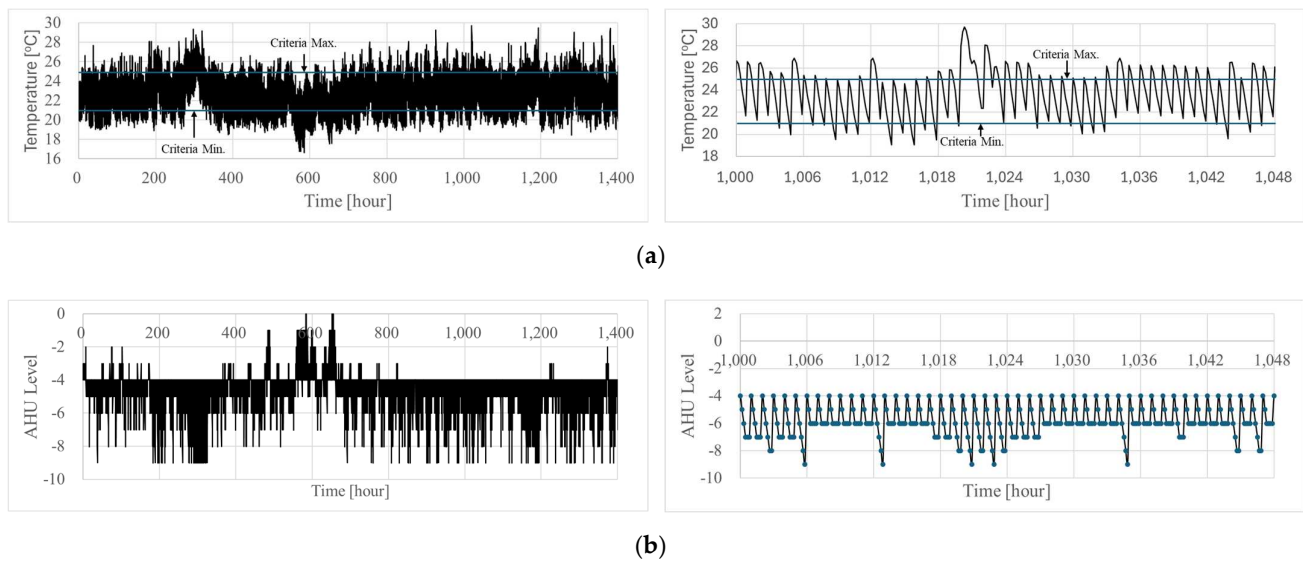


Figure 10. Results of applicability test of ROM in combination with HVAC system. (a) Variation of MCR temperature; (b) AHU Level variation controlled based on MCR temperature (Minus AHU Level: Cooling).

The first graph shows the temperature changes in the MCR over time. The temperature fluctuated within the range of approximately 16 °C to 30 °C, reflecting the temperature variations that occurred while the HVAC system was performing cooling and heating control. The “Criteria Max.” and “Criteria Min.” on the graph indicate the temperature maintenance criteria for the control room, representing the maximum and minimum allowable temperatures, respectively. This demonstrates that the system effectively controlled the temperature to stay within the set range. The enlarged graph on the right provides a detailed view of the temperature changes during a specific time period from 1000 h to 1048 h, showing that the temperature remained within the acceptable criteria throughout this period.

The second graph depicts how the cooling and heating performance of the Supply AHU is adjusted based on the MCR temperature. The AHU performance is indicated by negative values during cooling operations, signifying active cooling. Over time, the AHU performance fluctuates sharply, illustrating the system’s response to regulate temperature variations. The left graph shows that the AHU performance varied across a wide range throughout the entire simulation period, while the enlarged graph on the right details the specific control patterns during the time frame from 1000 h to 1048 h. During this period, the AHU performance responded rapidly to changes in the control room temperature, maintaining appropriate levels of control.

There is a time zone outside the temperature criteria set in Figure 10a, which can be explained by AHU control system logic and response time. When the temperature in the MCR deviates from the set criteria, the system adjusts the amount of seawater flowing into the AHU heat exchanger to regulate the air temperature supplied to the MCR. However, the time required to return the temperature to within the criteria depends on the control logic of the seawater flow valve, which is beyond the scope of this study. Despite some temporary deviations, the key point of this study is that the system automatically adjusts the AHU level to restore the temperature to the set criteria after a certain period. This confirms the developed ROM’s applicability in maintaining MCR temperature within acceptable limits in real time.

These results demonstrate that the integration of the control room HVAC system with the ROM effectively manages the control room temperature in response to various temperature conditions and load variations. Specifically, the maintenance of temperature within the allowable criteria and the corresponding adjustment of the Supply AHU’s cooling and heating performance validate the applicability of the system. This confirms that

the combined HVAC system and ROM can reliably control the control room temperature, ensuring safe and stable operation under diverse operating conditions.

6. Conclusions

In this study, a system integrating Digital Twin technology and Reduced Order Modeling (ROM) was developed to achieve real-time temperature control in the control room of a nuclear power plant, and its applicability was validated. To this end, Computational Fluid Dynamics (CFD) analyses were conducted to obtain the three-dimensional thermal flow distribution within the control room. Based on the accumulated CFD results under various operating conditions, a ROM was generated and validated. Furthermore, it was confirmed that the developed ROM, when combined with the HVAC system, effectively controls the control room temperature in real time.

The key achievements of this research are as follows. First, through CFD analyses, the thermal flow distribution within the control room under diverse operating conditions was precisely identified, demonstrating that the overall temperature distribution cannot be adequately represented by limited sensor data alone. Second, utilizing machine learning techniques, a ROM based on CFD data was successfully created, and it was verified that the generated ROM closely matched the CFD results with high precision. Notably, the ROM exhibited excellent predictive performance even for validation cases not included in the training dataset, thereby confirming its reliability under actual operating conditions. Third, in the real-time temperature control simulations integrating the ROM with the HVAC system, it was demonstrated that the control room temperature was stably maintained within the set criteria. This validated the effectiveness of the proposed Digital Twin-based control system.

This research presents the practical applicability of Digital Twin technology in high-safety systems such as nuclear power plants, showcasing its potential to enhance operational efficiency and safety through real-time monitoring and control. Specifically, the introduction of ROM significantly reduced the high computational costs and time associated with CFD analyses, enabling the implementation of real-time data processing and decision-support systems.

Future research should aim to further enhance the accuracy and versatility of the ROM by incorporating a wider range of operating conditions and additional sensor data through advanced training methodologies. Additionally, optimizing the interface for integration with real-time control systems and conducting pilot tests in actual operational environments will provide more concrete validation of the system's effectiveness. Moreover, leveraging advancements in artificial intelligence (AI) and machine learning techniques to continuously improve the ROM's predictive performance and expanding the application scope of Digital Twin technology will contribute to the optimization of operations in high-safety systems, including nuclear power plants.

In summary, this study presents an innovative approach for real-time temperature control in the control room of a nuclear power plant and confirms the feasibility of implementing an efficient and reliable control system through the integration of Digital Twin and ROM. This approach is expected to form a crucial foundation for maximizing safety and operational efficiency in various industrial settings, including nuclear power plants.

Author Contributions: Conceptualization, S.-H.K.; ROM generation and validation, D.-K.C.; CFD analysis, S.-M.S.; project administration, C.C.; writing—original draft preparation, S.-H.K.; writing—review and editing, C.C. All authors have read and agreed to the published version of the manuscript.

Funding: This research was funded by the Technology Development Program (S3323979) of the Ministry of SMEs and Startups (MSS, Korea).

Data Availability Statement: The data presented in this study are available on request from the corresponding author. The data are not publicly available due to design information security.

Acknowledgments: This work was supported by the Technology Development Program (S3323979) funded by the Ministry of SMEs and Startups (MSS, Korea).

Conflicts of Interest: All authors were employed by the company ELSOLTEC. The authors declare that the research was conducted in the absence of any commercial or financial relationships that could be construed as a potential conflict of interest. The authors declare that this study received funding from Ministry of SMEs and Startups. The funder was not involved in the study design, collection, analysis, interpretation of data, the writing of this article or the decision to submit it for publication.

References

1. Juárez, M.; Inglada, V.J.; Giret, A. Digital Twins: Review and Challenges. *J. Comput. Inf. Sci. Eng.* **2021**, *21*, 030802. [CrossRef]
2. Pliuhin, V.; Sukhonos, M.; Biletskyi, I.; Plankovskyy, S.; Tsegelnyk, Y. Implementation Features of Local and Remote Technical Objects Digital Twins. In *IOP Conference Series: Earth and Environmental Science*; IOP Publishing: Bristol, UK, 2024; Volume 1376. [CrossRef]
3. Mitkov, R.; Pantusheva, M.; Petrova-Antonova, D.; Naserentin, V.; Logg, A. The Role of Computational Fluid Dynamics within City Digital Twins: Opportunities and Challenges. *ISPRS Ann. Photogramm. Remote Sens. Spat. Inf. Sci.* **2024**, *10*, 131–136. [CrossRef]
4. Rozza, G.; Stabile, G.; Ballarin, F. (Eds.) *Advanced Reduced Order Methods and Applications in Computational Fluid Dynamics*; Society for Industrial and Applied Mathematics: Philadelphia, PA, USA, 2022. [CrossRef]
5. Holemans, T.; Yang, Z.; Vanierschot, M. Efficient Reduced Order Modeling of Large Data Sets Obtained from CFD Simulations. *Fluids* **2022**, *7*, 110. [CrossRef]
6. Es-haghi, M.S.; Anitescu, C.; Rabczuk, T. Methods for Enabling Real-Time Analysis in Digital Twins: A Literature Review. *Comput. Struct.* **2024**, *297*, 107342. [CrossRef]
7. Wang, H.; Cao, Y.; Huang, Z.; Liu, Y.; Hu, P.; Luo, X.; Song, Z.; Zhao, W.; Liu, J.; Sun, J.; et al. Recent Advances on Machine Learning for Computational Fluid Dynamics: A Survey. *arXiv* **2023**, arXiv:2408.12171.
8. Costa, A.; Alba, M.; Biancolini, M. Geometric and Physical Reduced Order Modeling Applied to CFD Results. 2022. Available online: <https://engrxiv.org/preprint/view/2545> (accessed on 13 September 2022).
9. Aversano, G.; Ferrarotti, M.; Parente, A. Digital Twin of a Combustion Furnace Operating in Flameless Conditions: Reduced-Order Model Development from CFD Simulations. *Proc. Combust. Inst.* **2021**, *38*, 5373–5381. [CrossRef]
10. Wijesooriya, K.; Mohotti, D.; Lee, C.-K.; Mendis, P. A Technical Review of Computational Fluid Dynamics (CFD) Applications on Wind Design of Tall Buildings and Structures: Past, Present and Future. *J. Build. Eng.* **2023**, *74*, 106828. [CrossRef]
11. Huang, B.; Hui, Y.; Liu, Y.; Wang, H. Design of Twin Builder-Based Digital Twin Online Monitoring System for Crane Girders. *Sensors* **2023**, *23*, 9203. [CrossRef]
12. KEPCO; KHNP. APR1400 Standard Design Certification Application Design Control Document, Revision 3, Tier 1 and Tier 2. Available online: <https://www.nrc.gov/reactors/new-reactors/large-lwr/design-cert/apr1400/dcd.html> (accessed on 26 September 2024).
13. International Atomic Energy Agency. *Modern Instrument and Control for Nuclear Power Plants: A Guidebook, Technical Reports Series No. 387*; International Atomic Energy Agency: Vienna, Austria, 1999.
14. International Atomic Energy Agency. *Control Room Systems Design for Nuclear Power Plants, IAEA-TECDOC-812*; International Atomic Energy Agency: Vienna, Austria, 1995.
15. Jung, Y.-S.; Cho, S.-J. Development of a Prototype for the Digitalized Nuclear Power Plant's Main Control Room. *J. Inst. Internet Broadcast Commun.* **2009**, *9*, 145–152.
16. Kim, D.W. A Comparative Study of Evacuation Scenario of the Auxiliary Building's Main Control Room in Nuclear Power Plants. Master's Thesis, Hanyang University, Seoul, Republic of Korea, 2015.
17. International Atomic Energy Agency. *Instrumentation and Control Systems for Advanced Small Modular Reactors, IAEA Nuclear Energy Series, No. NP-T-3.19*; International Atomic Energy Agency: Vienna, Austria, 2017.
18. International Atomic Energy Agency. *Core Knowledge on Instrumentation and Control Systems in Nuclear Power Plants, IAEA Nuclear Energy Series, No. NP-T-3.12*; International Atomic Energy Agency: Vienna, Austria, 2011.
19. U.S. Nuclear Regulatory Commission. *Instrumentation and Controls in Nuclear Power Plants: An Emerging Technologies Update, NU-REG/CR-6992*; U.S. Nuclear Regulatory Commission: Washington, DC, USA, 2009.
20. Choi, J.; Kim, H.; Jung, W.; Lee, S.J. Analysis of Interface Management Tasks in a Digital Main Control Room. *Nucl. Eng. Technol.* **2019**, *51*, 1554–1560. [CrossRef]
21. Lee, M.S.; Hong, J.H.; Suh, J.K.; Lee, S.H.; Hwang, D.H. Development of Human Factors Validation System for the Advanced Control Room of APR1400. *J. Nucl. Sci. Technol.* **2009**, *46*, 90–101. [CrossRef]
22. Kim, B.; Lee, J.; Kim, S.; Shin, W.G. Habitability Evaluation Considering Various Input Parameters for Main Control Benchboard Fire in the Main Control Room. *Nucl. Eng. Technol.* **2022**, *54*, 4195–4208. [CrossRef]
23. Patankar, S.V.; Spalding, D.B. A Calculation Procedure for Heat, Mass and Momentum Transfer in Three-Dimensional Parabolic Flows. *Int. J. Heat Mass Transf.* **1972**, *15*, 1787–1806. [CrossRef]
24. ANSYS, Inc. *ANSYS Fluent Theory Guide*; ANSYS, Inc.: Canonsburg, PA, USA, 2023.
25. ANSYS, Inc. *ANSYS Fluent User's Guide*; ANSYS, Inc.: Canonsburg, PA, USA, 2023.
26. Carlberg, K.; Farhat, C.; Cortial, J.; Amsallem, D. The GNAT Method for Nonlinear Model Reduction: Effective Implementation and Application to Computational Fluid Dynamics and Turbulent Flows. *J. Comput. Phys.* **2013**, *242*, 623–647. [CrossRef]

-
27. Salem, M.B.; Gogu, C.; Haftka, R.T. Automatic Selection for General Surrogate Models. *Struct. Multidiscip. Optim.* **2018**, *58*, 719–734. [[CrossRef](#)]
 28. ANSYS, Inc. *Twin Builder Help, Release 2023R1*; ANSYS, Inc.: Canonsburg, PA, USA, 2023.

Disclaimer/Publisher’s Note: The statements, opinions and data contained in all publications are solely those of the individual author(s) and contributor(s) and not of MDPI and/or the editor(s). MDPI and/or the editor(s) disclaim responsibility for any injury to people or property resulting from any ideas, methods, instructions or products referred to in the content.